Trend detection in satellite observations of formaldehyde tropospheric columns

I. De Smedt,[1] T. Stavrakou,[1] J.-F. Müller,[1] R. J. van der A,[2] and M. Van Roozendael[1]

Received 8 June 2010; revised 29 July 2010; accepted 6 August 2010; published 22 September 2010.

[1] Being an intermediate product in the oxidation of a large number of non-methane volatile organic compounds (NMVOCs), formaldehyde (H_2CO) is a useful indicator of biogenic, pyrogenic and anthropogenic hydrocarbon emissions. We present the first trend study performed on H_2CO satellite columns, retrieved from the GOME and SCIAMACHY instruments between 1997 and 2009. A linear model with a seasonal component is used to fit the time series of monthly averaged columns. The error and statistical significance of the inferred trends are estimated. The study focuses on Asia but results are also provided for large cities worldwide. Statistically significant positive trends of formaldehyde columns are observed over northeastern China (4% yr^{-1}) and India (1.6% yr^{-1}), related to strong increases in anthropogenic NMVOC emissions, whereas negative trends of about −3% yr^{-1} are observed over Tokyo as well as over cities of the northeast U.S. urban corridor as a result of effective pollution regulation measures. **Citation:** De Smedt, I., T. Stavrakou, J.-F. Müller, R. J. van der A, and M. Van Roozendael (2010), Trend detection in satellite observations of formaldehyde tropospheric columns, *Geophys. Res. Lett.*, *37*, L18808, doi:10.1029/2010GL044245.

1. Introduction

[2] Non-methane volatile organic compounds (NMVOCs) play an important role in tropospheric chemistry and air quality because they participate to the formation of tropospheric ozone (in the presence of nitrogen oxides), and secondary organic aerosols [*Houweling et al.*, 1998; *Kanakidou et al.*, 2005]. Formaldehyde (H_2CO) is a short-lived oxidation product of a large number of NMVOCs emitted either naturally or by human activities. Satellite observations of H_2CO columns have been used to constrain biogenic and biomass burning NMVOC emissions [*Palmer et al.*, 2003, 2006; *Fu et al.*, 2007; *Stavrakou et al.*, 2009a, 2009b; *Barkley et al.*, 2009], as well as anthropogenic NMVOC emissions [*Fu et al.*, 2007].

[3] In this work, we take advantage of the 13-year long GOME-SCIAMACHY record [*De Smedt et al.*, 2008] to estimate trends and relate them to changes in anthropogenic NMVOC emissions using the IMAGESv2 global chemistry transport model [*Stavrakou et al.*, 2009a]. Our approach follows the method of *van der A et al.* [2006, 2008], used for the determination of trends in satellite NO_2 observations. Our main focus is on Asia, where the rapid growth of economic activity during the last decades resulted in large increases of anthropogenic emissions, but results for world megacities are also discussed.

2. Satellite Observations

[4] A combination of H_2CO columns retrieved from GOME/ERS-2 (1997–2002) and from SCIAMACHY/ENVISAT (2003–2009) is used in this study. A complete description of the retrieval, based on the DOAS method, is provided by *De Smedt et al.* [2008]. Slant columns (SC) are fitted in the 328.5–346 nm spectral range. Air mass factors (AMFs) are calculated using scattering weights evaluated from radiative transfer simulations performed with the LIDORT v3.3 code [*Spurr*, 2008]. Daily *a priori* H_2CO vertical profiles are obtained from the IMAGESv2 model [*Stavrakou et al.*, 2009a]. Clouds are treated in the independent pixel approximation using FRESCO+ parameters [*Wang et al.*, 2008]. Observations with cloud fractions larger than 40% are filtered out. No explicit correction is applied for aerosols but the cloud correction scheme accounts for a large part of the aerosol scattering effect [*De Smedt et al.*, 2008]. An estimation of the random and systematic error budget is provided for each pixel. The total error on the monthly and regionally averaged columns is comprised between 20 and 40%. The detection limit is 2×10^{15} molec.cm^{-2}. Compared to *De Smedt et al.* [2008], several improvements have been introduced. First, a unique set of high-resolution cross-sections is used for both instruments [*De Smedt et al.*, 2009], among them the recommended H_2CO absorption cross sections of *Meller and Moortgat* [2000]. Second, to reduce the errors associated to topography, scattering weights are calculated with a finer altitude grid near the ground and the *a priori* profiles are rescaled to the ground altitude following *Zhou et al.* [2009]. The new AMFs are generally larger by less than 5% except over high altitude plateaus where the differences can reach 20%. Figure 1 (top) shows the mean H_2CO vertical columns (VC) over Asia as retrieved from GOME between 1997 and 2002 and from SCIAMACHY between 2003 and 2009. Due to the decreasing sensitivity of tropospheric retrievals with increasing solar zenith angle, only columns for SZA lower than 60° are accounted.

3. Trend Analysis Method

[5] We fit the time series of monthly observations using a model with a linear trend and a seasonal component [*van der A et al.*, 2006]: $m(t) = A + Bt + \sum_{n=1}^{4} C_n \cos(n2\pi t) + \sum_{n=1}^{4} D_n \sin(n2\pi t) + U\delta$, where $m(t)$ is the observed monthly H_2CO VC for month t (expressed in fractional year), and A,

[1]Belgian Institute for Space Aeronomy, Brussels, Belgium.
[2]Royal Netherlands Meteorological Institute, De Bilt, Netherlands.

0094-8276/10/2010GL044245

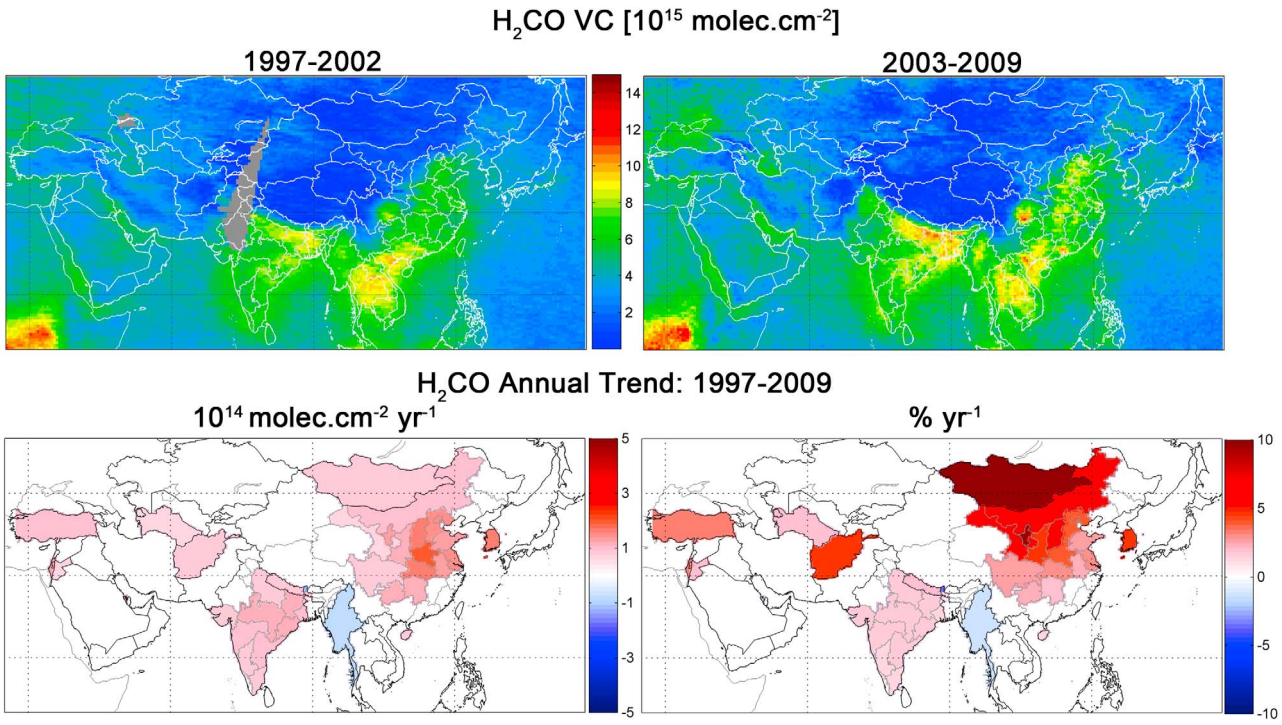

Figure 1. Mean H_2CO VC from GOME (top left) and SCIAMACHY (top right). Absolute (bottom left) and relative (bottom right) annual trends over 1997–2009. The relative trends are calculated with 1997 as reference year. Blank areas represent not statistically significant results.

B, C_n, D_n and U are the fitted parameters. A is the annual mean of the first year, B is the annual trend, expressed in molec.cm^{-2} yr^{-1}, C_n and D_n are the Fourier terms used to model the seasonal variations. U accounts for a possible bias between the GOME and SCIAMACHY retrievals (δ switches from 0 to 1 in Jan. 2003). A linear least-squares method is used to fit the function with the observations, taking their errors into account. In order to assess the statistical significance of the derived annual trends, the uncertainties on the fitted parameters are provided by the bootstrap resampling method [*Gardiner et al.*, 2008]. This technique enables to treat non-normally distributed data and is designed to accommodate for outliers, while providing uncertainties comparable with least-squares estimates when a Gaussian model is appropriate. The difference between the lower and the upper confidence limits of the inferred trend (the 2.5% and 97.5% quantiles) is equivalent to the standard deviation ($2\sigma_B$) for normal distributions [*Gardiner et al.*, 2008]. The significance level of the trend is better than 95% for $t_B = |B/\sigma_B|$ larger than 2 [*Weatherhead et al.*, 1998; *van der A et al.*, 2006]. The derived absolute trends between 1997 and 2009 over Asian countries and the corresponding growth rates relative to 1997 are shown on Figure 1 (bottom), whereas examples of monthly averaged H_2CO observations and fitted time series in India and northeastern China are shown on Figure 2. The magnitude of the fitted offset U is found to be lower than 1.5×10^{15} molec.cm^{-2}, which is smaller than the minimum error on the observations.

4. Results

[6] We present trend analysis results for China, India, other Asian countries, as well as for world megacities, where the trends are statistically significant. A complete list of the trends distributed by Asian country, Chinese province, Indian state, and the most important agglomerations worldwide, is provided in the auxiliary material.[1]

4.1. China

[7] Over China, the inferred annual trend is $0.8 \pm 0.2 \times 10^{14}$ molec.cm^{-2} yr^{-1} ($3 \pm 0.8\%$ yr^{-1} between 1997 and 2009). As seen on Figure 1 and in Table S2 of the auxiliary material, the largest absolute trends (1.5×10^{14} molec.cm^{-2} yr^{-1}) are found in the northeastern part of the country, i.e., in the region with the highest anthropogenic emissions [*Ohara et al.*, 2007]. Figure 2 (bottom) shows the H_2CO trend in the Beijing-Tianjin-Hebei area, where the growth rate is $4 \pm 1.4\%$ yr^{-1}. In northern China, the sparsely populated province of Inner Mongolia shows a strong trend of $6.4 \pm 2.8\%$ yr^{-1} between 1997 and 2009, whereas the Ningxia province, bordering Inner Mongolia, has the highest relative trend of $9.7 \pm 4.1\%$ yr^{-1}, indicative of a very fast industrial development most likely related to the construction of new power plants [*Zhang et al.*, 2009].

[8] Based on geographic and economic criteria, the 31 Chinese provinces can be grouped into six distinct regions [*Cai and Xie*, 2009]. The time series of both the annual and winter means of the regionally averaged columns are shown on Figure 3 and the corresponding trend values are provided in Table 1. The increasing trend of the annual means is significant in almost all regions. The highest growth rate ($5.5 \pm 2.2\%$ yr^{-1}) is found in the northwestern region

[1] Auxiliary materials are available in the HTML. doi:10.1029/2010GL044245.

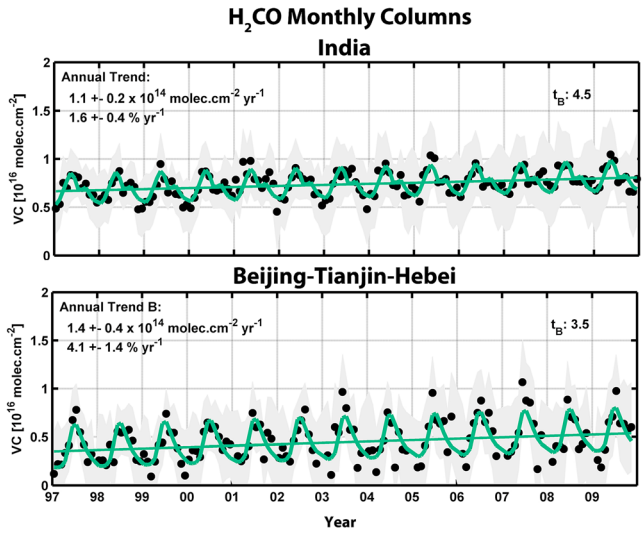

Figure 2. Measured (black dots) and fitted (green line) time series of H_2CO columns over India (top) and the Beijing-Tianjin-Hebei area in China (bottom).

(mainly driven by the Shaanxi and Ningxia provinces), followed by the northern and central regions. When considering only the October to March period, when the contribution of natural sources of H_2CO precursors is lowest, the trend is much stronger, particularly in northern China. For example, although the northeastern region presents a very weak annual trend, it exhibits a strong trend of 5.7 ± 2.5% yr^{-1} in the Oct.–Mar. period. Similarly, the trend in the northern region increases from 2.8 to 7.2% yr^{-1}, pointing to changes in anthropogenic NMVOC emissions.

[9] A trend of 5.1% yr^{-1} in the Chinese anthropogenic NMVOC emissions between 1997 and 2009 is reported in the REAS inventory (Regional Emission inventory in ASia), representing a total increase of 61% over this period [*Ohara et al.*, 2007]. Simulations performed with the IMAGESv2 model [*Stavrakou et al.*, 2009a] using the REAS NMVOC emission inventory for 1997 and 2009 show that the REAS emission trend leads to a total increase of 17–25% on the modeled H_2CO columns in eastern China (25–34% in winter), which is much lower than the observed increase of 40 ± 13% of the satellite H_2CO columns in the northern region of Figure 3 between 1997 and 2009. This result is most likely pointing to an underestimation of the reported REAS NMVOC emission trend. A similar underestimation of the NOx emission in REAS (by a factor of 2–4) has been reported by *Uno et al.* [2007], based on GOME NO_2 observations [*Richter et al.*, 2005]. A stronger increase in Chinese anthropogenic NMVOC emissions of 108% between 1997 and 2009, reported by *Bo et al.* [2008], is mostly attributed to an increase of the emissions due to traffic (particularly motorcycles), fossil fuel combustion and industrial processes. Further, the heavy industrialization of the coastal areas tends to expand towards central and northwestern inland regions, due to the transfer of emission-intensive plants from cities to rural areas with much less stringent pollution controls, coupled to the fact that fuel emission regulations are mainly implemented in the cities, which causes the transfer of the cheaper high emission vehicles to underdeveloped regions [*Bo et al.*, 2008; *Cai and Xie*, 2009].

[10] To make sure that the observed trends are not due to an indirect effect of aerosols, additional trend studies were performed on the cloud fractions and on the air mass factors used in the retrieval. No significant trend was found for

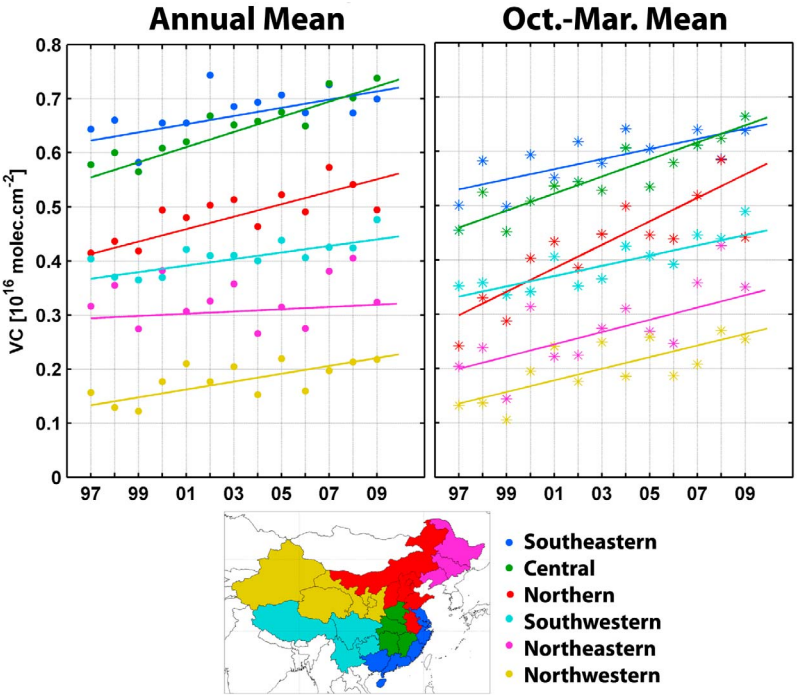

Figure 3. H_2CO annual and winter trends in 6 regions of China.

these parameters, confirming the actual increase of the tropospheric H_2CO columns [*van der A et al.*, 2006].

4.2. India and Other Asian Countries

[11] Over India, we find an annual trend of $1.1 \pm 0.2 \times 10^{14}$ molec.cm^{-2} yr^{-1}, which represents a growth rate of $1.6 \pm 0.4\%$ yr^{-1} (Figure 2). The country presents spatially homogeneous trends, with increasing H_2CO columns over almost all states, except for the northwestern states where trend analysis is not conclusive due to the systematic lack of GOME observations (Figure 1). The highest annual trend is observed around New Delhi ($1.8 \pm 0.6\%$ yr^{-1}), whereas slightly lower trends are found in the central states of Madhya Pradesh, Andhra Pradesh and Maharashtra, including Bombay (1.6% yr^{-1}) and in the northeastern states of Orissa and West Bengal, including Calcutta (1.6 and 1.3% yr^{-1}).

[12] In other Asian countries, significant trends are found over South Korea (4.5% yr^{-1}), Turkey (3.4% yr^{-1}), Israel (3.2% yr^{-1}) and Jordan (2% yr^{-1}). The largest annual growth rate is found in Mongolia ($22 \pm 18.6\%$ yr^{-1}) but the related uncertainty is large because of the low H_2CO columns in 1997. Countries like Afghanistan, Turkmenistan and Nepal present also statistically significant positive trends (Figure 1). A negative trend is found in Myanmar (−1.3% yr^{-1}). Thailand exhibits no trend while it presents the highest annual H_2CO columns, dominated by biogenic sources and biomass burning.

4.3. Principal Agglomerations of the World

[13] We calculated trends in the H_2CO vertical columns over the largest agglomerations of the world, based on monthly averages of satellite observations within a radius of 200km around city centers. This radius allows including enough satellite pixels to ensure significant trend analysis. The results are summarized in Table 2. Over Tokyo, we find a significant negative trend of −3.1% yr^{-1}, while the trend is zero for the whole Japan. Large positive trends are found in Chinese and Indian megacities, as well as in the Asian megacities of Seoul, Jakarta, Cairo, Istanbul and Tehran. In the eastern United States, we find important negative trends of about −3% yr^{-1} over New York, Washington, Dallas, Philadelphia and Miami. More surprisingly, Los Angeles and San Francisco present annual growth rates of 2 and 4 % yr^{-1}. According to the US EPA National Emission Inventory (http://www.epa.gov/ttnchie1/trends), the US anthropogenic NMVOC emissions present a negative trend of about −2% yr^{-1} for the whole country. In Europe, while the EMEP centre on emission inventories reports negative trends in the anthropogenic NMVOC emissions of −3% yr^{-1} [http://www.ceip.at], the H_2CO column trends in the megacities of London and Paris are slightly negative but not statistically significant. This might be due to the poor quality of the satellite H_2CO columns in Europe resulting from the low sensitivity of the UV instruments in the troposphere at these latitudes, coupled to the rather weak local H_2CO concentrations compared to other regions at the same latitudes [*De Smedt et al.*, 2008].

Table 1. H_2CO Trends Between 1997 and 2009 for the Regions Shown on Figure 3[a]

Region	Annual Trend	Oct.–Mar. Trend
Southeastern	0.8 ± 0.3 (1.2 ± 0.5)	0.9 ± 0.3 (1.8 ± 0.7)
Central	1.4 ± 0.3 (2.5 ± 0.6)	1.6 ± 0.4 (3.4 ± 0.9)
Northern	1.2 ± 0.3 (2.8 ± 1.0)	2.2 ± 0.4 (7.2 ± 1.9)
Southwestern	0.6 ± 0.2 (1.6 ± 0.7)	0.9 ± 0.3 (2.8 ± 1.0)
Northeastern	0.2 ± 0.3 (0.7 ± 1.2)	1.1 ± 0.4 (5.7 ± 2.5)
Northwestern	0.7 ± 0.2 (5.5 ± 2.2)	1.1 ± 0.3 (7.9 ± 2.9)

[a]Absolute trends are in 10^{14} molec.cm^{-2} yr^{-1} and relative trends (in parentheses) are in % yr^{-1}.

Table 2. Inferred Trends in Selected Large Cities Worldwide

City (Country)	Annual Trend (10^{14} molec.cm^{-2} yr^{-1})	Growth Rate (% yr^{-1})
Tokyo (Japan)	−1.5 ± 0.6	−3.1 ± 1.4
Manila (Philippines)	−0.7 ± 0.3	−1.4 ± 0.6
Beijing (China)	1.3 ± 0.3	4.0 ± 1.2
Shanghai (China)	1.1 ± 0.5	1.9 ± 1.0
Delhi (India)	1.0 ± 0.4	1.6 ± 0.7
Bombay (India)	0.7 ± 0.3	1.2 ± 0.5
Seoul (South Korea)	0.7 ± 0.3	1.8 ± 1.0
Jakarta (Indonesia)	1.1 ± 0.3	1.9 ± 0.5
Cairo (Egypt)	1.1 ± 0.3	2.7 ± 0.9
Istanbul (Turkey)	0.8 ± 0.3	2.0 ± 0.9
Tehran (Iran)	1.0 ± 0.3	2.8 ± 1.1
Lagos (Nigeria)	1.7 ± 0.4	1.5 ± 0.4
Kinshasa (Congo)	1.4 ± 0.5	1.1 ± 0.5
Los Angeles (USA)	0.7 ± 0.3	2.2 ± 0.9
San Francisco (USA)	1.0 ± 0.3	4.3 ± 1.6
New York (USA)	−1.5 ± 0.8	−3.5 ± 2.4
Washington (USA)	−1.6 ± 0.6	−2.8 ± 1.3
Dallas (USA)	−1.0 ± 0.5	−1.6 ± 0.9
Philadelphia (USA)	−1.8 ± 0.6	−3.3 ± 1.6
Miami (USA)	−1.4 ± 0.3	−2.7 ± 0.7
London (UK)	−0.7 ± 0.5	−0.4 ± 2.1
Paris (France)	−0.2 ± 0.5	−0.3 ± 1.0

5. Conclusions

[14] A consolidated time series of tropospheric formaldehyde columns retrieved from GOME and SCIAMACHY observations between 1997 and 2009 has been used to determine trends over Asia and over large agglomerations of the world. Over China, the trend is larger in the northeastern part and reaches 4% yr^{-1} in the Beijing-Tianjin-Hebei area, whereas in the southeastern region the trend is lower (1.2% yr^{-1}). India exhibits spatially homogeneous trends ranging between 1.3 and 1.8% yr^{-1}. The detected trends in H_2CO columns are explained by changes in the corresponding anthropogenic NMVOC emissions. Simulations performed with the IMAGESv2 model suggest that the reported trend of the REAS NMVOC emission inventory in Asia might be largely underestimated, particularly in central-east China. Negative trends (−3% yr^{-1}) are found around Tokyo and several cities of eastern U.S., illustrating the effective policies of emission reduction in these countries.

[15] **Acknowledgments.** We thank T. Gardiner and A. Forbes for providing the bootstrap resampling scripts and R. Spurr for providing the LIDORT code. This work has been supported by the EU-FP6 AMFIC project, the ESA DUP/DUE TEMIS service and the ESA GSE PROMOTE project.

References

Barkley, M. P., P. I. Palmer, I. De Smedt, T. Karl, A. Guenther, and M. Van Roozendael (2009), Regulated large-scale annual shutdown of Amazonian isoprene emissions?, *Geophys. Res. Lett.*, *36*, L04803, doi:10.1029/2008GL036843.

Bo, Y., H. Cai, and S. D. Xie (2008), Spatial and temporal variation of historical anthropogenic NMVOCs emission inventories in China, *Atmos. Chem. Phys.*, *8*, 7297–7316.

Cai, H., and S. D. Xie (2009), Tempo-spatial variation of emission inventories of speciated volatile organic compounds from on-road vehicles in China, *Atmos. Chem. Phys.*, *9*, 6983–7002.

De Smedt, I., et al. (2008), Twelve years of global observation of formaldehyde in the troposphere using GOME and SCIAMACHY sensors, *Atmos. Chem. Phys.*, *8*, 4947–4963.

De Smedt, I., et al. (2009), H_2CO columns retrieved from GOME-2: First scientific results and progress towards the development of an operational product, paper presented at the 2009 EUMETSAT Meteorological Satellite Conference, Bath, U. K.

Fu, T.-M., D. J. Jacob, P. I. Palmer, K. Chance, Y. X. Wang, B. Barletta, D. R. Blake, J. C. Stanton, and M. J. Pilling (2007), Space-based formaldehyde measurements as constraints on volatile organic compound emissions in east and south Asia and implications for ozone, *J. Geophys. Res.*, *112*, D06312, doi:10.1029/2006JD007853.

Gardiner, T., et al. (2008), Trend analysis of greenhouse gases over Europe measured by a network of ground-based remote FTIR instruments, *Atmos. Chem. Phys.*, *8*, 6719–6727.

Houweling, S., F. Dentener, and J. Lelieveld (1998), The impact of nonmethane hydrocarbon compounds on tropospheric photochemistry, *J. Geophys. Res.*, *103*, 10,673–10,696, doi:10.1029/97JD03582.

Kanakidou, M., et al. (2005), Organic aerosol and global climate modelling: A review, *Atmos. Chem. Phys.*, *5*, 1053–1123.

Meller, R., and G. K. Moortgat (2000), Temperature dependence of the absorption cross sections of formaldehyde between 223 and 323 K in the wavelength range 225–375 nm, *J. Geophys. Res.*, *105*, 7089–7101.

Ohara, T., et al. (2007), An Asian emission inventory of anthropogenic emission sources for the period 1980–2020, *Atmos. Chem. Phys.*, *7*, 4419–4444.

Palmer, P. I., D. J. Jacob, A. M. Fiore, R. V. Martin, K. Chance, and T. P. Kurosu (2003), Mapping isoprene emissions over North America using formaldehyde column observations from space, *J. Geophys. Res.*, *108* (D6), 4180, doi:10.1029/2002JD002153.

Palmer, P. I., et al. (2006), Quantifying the seasonal and interannual variability of North American isoprene emissions using satellite observations of the formaldehyde column, *J. Geophys. Res.*, *111*, D12315, doi:10.1029/2005JD006689.

Richter, A., et al. (2005), Increase in tropospheric nitrogen dioxide over China observed from space, *Nature*, *437*, 129–132, doi:10.1038/nature04092.

Spurr, R. (2008), LIDORT and VLIDORT: Linearized pseudo-spherical scalar and vector discrete ordinate radiative transfer models for use in remote sensing retrieval problems, in *Light Scattering Reviews*, vol. 3, *Light Scattering and Reflection*, edited by A. A. Kokhanovsky, pp. 229–271, Springer, Berlin.

Stavrakou, T. et al. (2009a), Evaluating the performance of pyrogenic and biogenic emission inventories against one decade of space-based formaldehyde columns, *Atmos. Chem. Phys.*, *9*, 1037–1060.

Stavrakou, T., et al. (2009b), Global emissions of non-methane hydrocarbons deduced from SCIAMACHY formaldehyde columns through 2003–2006, *Atmos. Chem. Phys.*, *9*, 3663–3679.

Uno, I., et al. (2007), Systematic analysis of interannual and seasonal variations of model-simulated tropospheric NO_2 in Asia and comparison with GOME-satellite data, *Atmos. Chem. Phys.*, *7*, 1671–1681.

van der A, R. J., D. H. M. U. Peters, H. Eskes, K. F. Boersma, M. Van Roozendael, I. De Smedt, and H. M. Kelder (2006), Detection of the trend and seasonal variation in tropospheric NO_2 over China, *J. Geophys. Res.*, *111*, D12317,doi:10.1029/2005JD006594.

van der A, R. J., H. J. Eskes, K. F. Boersma, T. P. C. van Noije, M. Van Roozendael, I. De Smedt, D. H. M. U. Peters, and E. W. Meijer (2008), Trends, seasonal variability and dominant NOx source derived from a ten year record of NO_2 measured from space, *J. Geophys. Res.*, *113*, D04302, doi:10.1029/2007JD009021.

Wang, P., et al. (2008), FRESCO+: An improved O_2 A-band cloud retrieval algorithm for tropospheric trace gas retrievals, *Atmos. Chem. Phys.*, *8*, 6565–6576.

Weatherhead, E. C., et al. (1998), Factors affecting the detection of trends: Statistical considerations and applications to environmental data, *J. Geophys. Res.*, *103*, 17,149–17,161.

Zhang, Q., D. G. Streets, and K. He (2009), Satellite observations of recent power plant construction in Inner Mongolia, China, *Geophys. Res. Lett.*, *36*, L15809, doi:10.1029/2009GL038984.

Zhou, Y., et al. (2009), An improved tropospheric NO_2 retrieval for OMI observations in the vicinity of mountainous terrain, *Atmos. Meas. Tech.*, *2*, 401–416.

I. De Smedt, J.-F. Müller, T. Stavrakou, and M. Van Roozendael, Belgian Institute for Space Aeronomy, Av. Circulaire 3, B-1180 Brussels, Belgium. (isad@aeronomie.be)

R. J. van der A, Royal Netherlands Meteorological Institute, PO Box 201, NL-3730 AE De Bilt, Netherlands.